

Ab initio study on the effects of transition metal doping of Mg_2NiH_4

Michiel J. van Setten and Gilles A. de Wijs

*Electronic Structure of Materials, Institute for Molecules and Materials,
Faculty of Science, Radboud University Nijmegen,
Toernooiveld 1, 6525 ED Nijmegen, The Netherlands*

Geert Brocks

*Computational Materials Science, Faculty of Science and Technology and MESA+ Institute for Nanotechnology,
University of Twente, P.O. Box 217, 7500 AE Enschede, The Netherlands*

(Dated: July 4, 2018)

Mg_2NiH_4 is a promising hydrogen storage material with fast (de)hydrogenation kinetics. Its hydrogen desorption enthalpy, however, is too large for practical applications. In this paper we study the effects of transition metal doping by first-principles density functional theory calculations. We show that the hydrogen desorption enthalpy can be reduced by ~ 0.1 eV/ H_2 if one in eight Ni atoms is replaced by Cu or Fe. Replacing Ni by Co atoms, however, increases the hydrogen desorption enthalpy. We study the thermodynamic stability of the dopants in the hydrogenated and dehydrogenated phases. Doping with Co or Cu leads to marginally stable compounds, whereas doping with Fe leads to an unstable compound. The optical response of Mg_2NiH_4 is also substantially affected by doping. The optical gap in Mg_2NiH_4 is ~ 1.7 eV. Doping with Co, Fe or Cu leads to impurity bands that reduce the optical gap by up to 0.5 eV.

PACS numbers: 71.20.-b, 71.15.Nc, 61.72.Bb, 74.62.Dh

I. INTRODUCTION

The large scale application of hydrogen as a fuel depends on the development of materials that can store hydrogen in a dense form.¹ Magnesium based hydrides are interesting candidate materials for hydrogen storage, because magnesium has a low weight. The simplest hydride, MgH_2 , has a hydrogen storage capacity of 7.67 wt.%. It has, however, a high hydrogen desorption enthalpy, 0.77 eV per H_2 , and hence an equilibrium plateau pressure (10^{-7} bar) at room temperature that is too low for practical applications.² Moreover, the hydrogen desorption/absorption reactions of MgH_2/Mg suffer from kinetic barriers, which requires operating temperatures in excess of 570 K. Various magnesium alloys have been studied to improve the thermodynamics and kinetics of the hydrogen desorption/absorption reaction.^{3,4,5,6,7,8} Mg_2NiH_4 , which can store 3.6 wt.% of hydrogen, has been suggested as a candidate material, primarily because of its reasonably fast hydrogen desorption/absorption kinetics.^{9,10,11,12,13,14,15} Several theoretical studies have been dedicated to Mg_2NiH_4 .^{16,17,18,19,20} However, its measured hydrogen desorption enthalpy of 0.70 eV per H_2 ,¹⁴ is barely lower than that of MgH_2 . It leads to an equilibrium hydrogen pressure of 1 bar at 510 K.¹⁵ This temperature is far too high for applications using PEM fuel cells, for instance. Apart from its possible role in hydrogen storage, Mg_2Ni is also interesting because it can act switchable mirror.^{21,22,23,24} Mg_2Ni is a metal, whereas Mg_2NiH_4 is a semiconductor with a band gap of 1.7-2.0 eV.^{25,26,27} This leads to a remarkable change in the optical properties of the material upon hydrogenation and dehydrogenation. Especially if Mg_2Ni is applied in thin films, the optical switching can

be fast, reversible and robust.²⁸ The high optical contrast opens up possibilities for Mg_2Ni as a hydrogen sensing material.^{29,30,31}

For both applications the reaction enthalpy of the hydrogen desorption/absorption at typical operating conditions is too high. Preferable would be an equilibrium hydrogen pressure of 1 bar at room temperature. To reach this condition a hydrogen desorption enthalpy of 0.40 eV per H_2 is required. A substantial amount of experimental work has been dedicated to study the effects of doping of Mg_2NiH_4 in order to reduce its hydrogen desorption enthalpy.^{28,32,33,34,35,36,37,38,39,40,41} In this context “doping” means substituting a fairly large amount of Ni (or Mg) by other metals.

In this paper we report a study on the effects of doping Mg_2NiH_4 with transition metals by first principles density functional theory (DFT) calculations. We restrict ourselves to the LT phase of Mg_2NiH_4 , since the HT phase is stable only at elevated temperatures (i.e. $T > 500\text{K}$) and therefore less relevant for applications.¹⁴ We consider substitution of nickel by cobalt, iron, or copper in a concentration of 12.5%, which means substituting one in eight nickel atoms. This concentration is close to that used in recent experiments.⁴² Our first aim is to monitor the change in hydrogen desorption enthalpy and, in particular, to establish which dopants (if any) lead to a reduction of the enthalpy. We show that zero point energies (ZPEs) associated with the hydrogen phonon modes considerably influence the enthalpies. Our second objective is to study the change in optical properties that results from doping. In particular we show that dopants in this concentration markedly alter the dielectric function.

II. COMPUTATIONAL METHODS

First principles DFT calculations are carried out using a plane wave basis set and the projector augmented wave (PAW) method,^{43,44} as incorporated in the Vienna *Ab initio* Simulation Package (VASP),^{45,46,47}. We use the PW91 generalized gradient approximation (GGA) for the exchange correlation functional.⁴⁸ The cell parameters are kept at the experimental values and the atomic positions are relaxed using a conjugate gradient algorithm. Non-linear core corrections are applied.⁴⁹

To calculate accurate reaction enthalpies for reactions involving light elements such as hydrogen, it is essential to take into account the ZPE contribution. To calculate ZPEs we need the phonon frequencies of the materials involved. Phonon frequencies are calculated using a direct method,⁵⁰ i.e. the dynamical matrix is constructed from the force constants that are obtained from finite differences. Two opposite displacements of 0.05 Å are used for each atomic degree of freedom. In general one needs to carry out such calculations on a super cell containing several primitive unit cells, as the force constants do not go to zero within a distance corresponding to a single unit cell. However, the unit cells of the materials studied in this paper turn out to be sufficiently large, except for bulk magnesium, for which a $2 \times 2 \times 2$ super cell is used. An advantage of large unit cells is that the phonon dispersion is small. It is therefore sufficient to calculate ZPEs from the phonon frequencies obtained at Γ .

The dielectric functions are calculated in the or independent particle random phase approximation taking into account direct transitions from occupied to unoccupied Kohn-Sham orbitals only. We neglect excitonic, local field and quasi-particle effects. The imaginary part of the macroscopic dielectric function then has the form

$$\varepsilon^{(2)}(\hat{\mathbf{q}}, \omega) = \frac{8\pi^2 e^2}{V} \lim_{|\mathbf{q}| \rightarrow 0} \frac{1}{|\mathbf{q}|^2} \sum_{\mathbf{k}, v, c} \quad (1)$$

$$\times |\langle u_{c, \mathbf{k}+\mathbf{q}} | u_{v, \mathbf{k}} \rangle|^2 \delta(\epsilon_{c, \mathbf{k}+\mathbf{q}} - \epsilon_{v, \mathbf{k}} - \hbar\omega),$$

where $\hat{\mathbf{q}}$ gives the direction of \mathbf{q} ; v, \mathbf{k} and c, \mathbf{k} label single particle states that are occupied, unoccupied in the ground state, respectively; ϵ, u are the single particle energies and the translationally invariant parts of the wave functions, respectively; V is the volume of the unit cell. Further details can be found in Ref. 51.

Almost all experimental optical data on hydrides are obtained from micro- or nano-crystalline samples whose crystallites have a significant spread in orientation. The most relevant quantity then is the directionally averaged dielectric function, i.e., $\varepsilon^{(2)}(\omega)$ averaged over $\hat{\mathbf{q}}$. In this paper we only report directionally averaged dielectric functions.

The Brillouin zone integrations are performed using a modified tetrahedron method.⁵² All calculations on the hydrides use a $7 \times 7 \times 7$ Monkhorst-Pack \mathbf{k} -point mesh for sampling the Brillouin zone, and the calculations on the metals use a $7 \times 7 \times 3$ Monkhorst-Pack \mathbf{k} -point mesh.⁵³ We

use 480 bands to calculate the dielectric function. This number of bands includes all transitions up to 30 eV. For the materials containing copper a plane wave kinetic energy cutoff of 341 eV is used, and for the other materials a cutoff of 337 eV. To obtain accurate formation and reaction enthalpies, the total energies of all final structures are calculated using a plane wave kinetic energy cutoff of 700 eV.

III. STRUCTURE AND STABILITY OF UNDOPED MATERIALS: Mg_2NiH_4 , Mg_2CoH_5 , Mg_2FeH_6 , Mg_2Ni AND ELEMENTAL METALS

In order to assess the stability of doped Mg_2NiH_4 we first need the total energies of the undoped hydrides and of all elemental metals involved. The optimized structures of Mg_2NiH_4 , Mg_2CoH_5 , Mg_2FeH_6 are given in Table I. They are in good agreement with the experimental structures.^{54,55,56} The metal atoms in LT Mg_2NiH_4 form a distorted CaF_2 -type structure. Four hydrogen atoms are arranged around each nickel atom in a tetrahedron. In Mg_2FeH_6 and Mg_2CoH_5 the Mg and Fe/Co atoms form an undistorted CaF_2 -type structure. In Mg_2FeH_6 the hydrogen atoms form regular octaeders around the iron atoms. In Mg_2CoH_5 the hydrogen atoms occupy five corners of a slightly distorted octahedron around each cobalt atom.

The experimental structure of Mg_2Ni can be found in Ref. 12. The unit cell contains 12 Mg and 6 Ni atoms, which are basically hexagonally closed packed. The optimized structure given in Table I is in good agreement with experiment. For MgH_2 we use a previously calculated structure.⁵⁷ For the elemental metals and MgCu_2 we use the experimental lattice parameters, i.e., $a(c) = 3.21(5.21)$ Å, $a = 2.87$ Å, $a(c) = 2.51(4.07)$ Å, $a = 3.52$ Å $a = 3.61$ Å and $a = 7.03$ Å for Mg, Fe, Co, Ni, Cu and MgCu_2 , respectively.⁵⁸ The magnetic elements iron, cobalt and nickel are treated by spin-polarized calculations. The calculated pressures are small, indicating that it is unnecessary to explicitly optimize the lattice parameters. We explicitly tested the latter for iron, since there the external pressure was largest, and obtained an energy gain of less than 0.01 eV.

In order to obtain accurate enthalpies for reactions involving materials that contain hydrogen, one has to take ZPEs into account. All calculated total energies and ZPEs are given in Table II. We neglect the ZPEs of the elemental metals. The ZPE for magnesium is only 0.001 eV/atom. The ZPEs iron, cobalt, nickel and copper will be even smaller, since the atomic weight of those elements is more than twice that of Mg. We did not calculate the ZPEs for Mg_2FeH_6 and Mg_2CoH_5 , since we use these compounds only to study the stability of doped Mg_2NiH_4 with respect to phase segregation, where the ZPE corrections are rather small.

To calculate hydrogen desorption enthalpies we also need the total energy of the hydrogen molecule. It is cal-

TABLE I: Calculated atomic positions of Mg_2NiH_4 (exp. Ref. 54), Mg_2CoH_5 (exp. Ref. 55), Mg_2FeH_6 (exp. Ref. 56) and Mg_2Ni (exp. Ref. 12). In the calculations the lattice parameters were kept at the experimental values.

Compound	Space group unit cell		x	y	z
Mg_2NiH_4	C2/c (15)	Mg 8f	0.2646	0.4863	0.0833
	$\beta = 113.52^\circ$	Mg 4e	0	0.0252	0.2500
	$a = 14.343 \text{ \AA}$	Mg 4e	0	0.5264	0.2500
	$b = 6.4038 \text{ \AA}$	Ni 8f	0.1199	0.2294	0.0801
	$c = 6.4830 \text{ \AA}$	H 8f	0.2088	0.3048	0.3041
		H 8f	0.1390	0.3192	0.8760
		H 8f	0.0096	0.2908	0.0527
		H 8f	0.1243	0.9866	0.0727
Mg_2CoH_5	P4/nmm (129)	Mg 2a	3/4	1/4	0
	$a = 4.463 \text{ \AA}$	Mg 2b	3/4	1/4	1/2
	$c = 6.593 \text{ \AA}$	Co 2c	1/4	1/4	0.2567
		H 2c	1/4	1/4	0.4947
		H 8j	0.4914	0.4914	0.2268
Mg_2FeH_6	Fm3m (225)	Mg 8c	1/4	1/4	1/4
	$a = 6.437 \text{ \AA}$	Fe 4a	0	0	0
		H 24e	0.2425	0	0
Mg_2Ni	P6 ₃ 22 (180)	Mg 6i	0.1639	0.3278	0
	$\gamma = 120^\circ$	Mg 6f	1/2	0	0.1165
	$a = 5.205 \text{ \AA}$	Ni 3b	0	0	1/2
	$c = 13.236 \text{ \AA}$	Ni 3d	1/2	0	1/2

culated using a cubic cell with sides of 13 Å. We find an equilibrium distance of 0.7486 Å, a vibrational frequency of 4350 cm^{-1} and a dissociation energy of 4.57 eV, which compare reasonably well with the experimental values of 0.7461 Å, 4401 cm^{-1} and 4.48 eV, respectively.^{58,59} The 0.1 eV deviation in the dissociation energy of H_2 is relatively large in view of the accuracy required for calculating hydrogen desorption enthalpies. This 0.1 eV may be considered as a correction to the reaction enthalpies discussed below.

We calculate the ZPE for the hydrogen molecule from the energy levels of a Morse potential,

$$E(n) = \hbar\omega \left(n + \frac{1}{2} \right) - \frac{1}{4D_e} \left[\hbar\omega \left(n + \frac{1}{2} \right) \right]^2, \quad (2)$$

where ω is the vibration frequency and D_e is the dissociation energy. The result is given in Table II.

IV. DOPED Mg_2NiH_4 AND Mg_2Ni

A. Structure

The unit cell of the LT phase of Mg_2NiH_4 contains eight formula units. To simulate doping we replace one of the Ni atoms by a Fe, Co, or Cu atom, thus achieving a 7:1 ratio between Ni and dopant atoms. In simple terms

TABLE II: Calculated total energies and ZPEs of the undoped hydrides and metals per formula unit.

	E (eV)	ZPE (eV)		E (eV)	ZPE (eV)
H_2	-6.803	0.266	MgH_2	-8.983	
Mg	-1.524	0.001	Mg_2Ni	-9.133	0.102
Fe	-8.150		Mg_2FeH_6	-34.511	
Co	-6.841		Mg_2CoH_5	-29.355	
Ni	-5.459		Mg_2NiH_4	-24.053	0.852
Cu	-3.725		MgCu_2	-9.45	

one can think of undoped Mg_2NiH_4 as being constructed from Mg^{2+} and $(\text{NiH}_4)^{4-}$ ions. The latter involve 18 valence electrons and are closed shell ions. Upon doping it is likely that in the fully hydrogenated phase the closed shell character is maintained. This means that $(\text{NiH}_4)^{4-}$ is replaced by $(\text{FeH}_6)^{4-}$, $(\text{CoH}_5)^{4-}$, or $(\text{CuH}_3)^{4-}$. Thus for a Fe atom we add two extra hydrogen atoms, for a Co atom one and for a Cu atom we remove one hydrogen atom. For all doped systems we fix the unit cell to that of undoped Mg_2NiH_4 and we optimize the atomic positions. The external pressures on the doped systems are small, which indicates that the gain in energy when relaxing the cell volumes will not be significant.

The geometry of the hydrogens around the Fe and Co dopant atoms resembles the geometry in Mg_2FeH_6 and Mg_2CoH_5 respectively. In Mg_2FeH_6 each Fe atom is in the center of a perfect octahedron of hydrogen atoms with a Fe-H distance of 1.56 Å. In Fe doped Mg_2NiH_4 the octahedron is distorted. The H-Fe-H angles range from 80 to 100° and the Fe-H distances range from 1.55 to 1.58 Å in case a H atom is only bonded to a Fe atom. However, four of the hydrogen atoms surrounding a Fe atom also bond to Ni atoms, in which case the Fe-H distance is enlarged to 1.64–1.76 Å. The hydrogen tetrahedra around such Ni atoms are distorted with Ni-H distances from 1.51 to 1.80 Å, whereas in undoped Mg_2NiH_4 they are between 1.56 and 1.58 Å.

In the case of Co doping the distortions are much smaller. In Mg_2CoH_5 the hydrogen atoms surrounding each Co atom form a four-sided pyramid with the Co atom just above the basal plane of the pyramid. To describe the geometry we denoting the basal plane hydrogens by H_b and the top hydrogen by H_t . The H_b -Co- H_b angle is 89°, the Co- H_b distance is 1.52 Å, the H_b -Co- H_t angle is 97.6° and the Co- H_t distance is 1.59 Å. The Co-Mg distances range from 2.75 to 2.80 Å. The hydrogens surrounding the Co atom in doped Mg_2NiH_4 form a slightly distorted pyramid, with H_b -Co- H_b angles ranging from 83.1° to 94.1° and Co- H_b distances ranging from 1.53 to 1.56 Å. The H_b -Co- H_t angle is 93.4° to 105.1° and the Co- H_t distance is 1.57 Å. The Co-Mg distances vary from 2.69 to 2.80 Å. The Ni-H bond lengths are not affected by Co doping.

We cannot compare the geometry of the hydrogens in Cu doped Mg_2NiH_4 to Mg_2CuH_3 , since the latter compound is not stable with respect to decomposition into

TABLE III: Calculated total energies, ZPEs and hydrogen content of the doped hydrides, $\text{Mg}_2\text{Ni}_{7/8}\text{TM}_{1/8}\text{H}_x$, and the metals, $\text{Mg}_2\text{Ni}_{7/8}\text{TM}_{1/8}$. The values are per formula unit.

TM	E (eV)	ZPE (eV)	x (#H)
Fe	-24.952	0.914	4.250
Co	-24.677	0.876	4.125
Ni	-24.053	0.852	4.000
Cu	-23.207	0.826	3.875
Fe	-9.278	0.100	
Co	-9.233	0.100	
Ni	-9.133	0.102	
Cu	-8.890	0.102	

MgH_2 and MgCu_2 .³² The Ni-H distances in Cu doped Mg_2NiH_4 are similar to those in undoped Mg_2NiH_4 . The hydrogen atoms surrounding the Cu atom are located at three corners of a tetrahedron with the Cu atom in the center. The Cu-H distances, 1.62 to 1.64 Å, are slightly larger than the Ni-H distances, 1.56 to 1.59 Å.

B. Reaction enthalpies

In order to calculate the hydrogen desorption enthalpy of doped Mg_2NiH_4 we also need the total energy of doped Mg_2Ni . The unit cell of Mg_2Ni contains six formula units per cell. If we replace one of the Ni atoms in this cell by a dopant atom, this gives a 5:1 Ni:dopant ratio, instead of the required 7:1 ratio. We approximate the total energy of the 7:1 ratio by the average energy of three 5:1 doped unit cells and one undoped cell. All calculated total energies and ZPEs of the doped hydrides and metals are given in Table III.

From the data in Table III we calculate the desorption enthalpy per H_2 molecule

$$E_{\text{des}} = E(\text{H}_2) + \frac{2}{x} \left[E(\text{Mg}_2\text{Ni}_{7/8}\text{TM}_{1/8}) - E(\text{Mg}_2\text{Ni}_{7/8}\text{TM}_{1/8}\text{H}_x) \right], \quad (3)$$

where $E(\text{M})$ is the total energy of compound M and x is the number of hydrogen atoms in the hydride. The latter depends upon the dopant atom, as discussed in the previous section. The values of x are given in Table III.

The calculated desorption enthalpy of undoped Mg_2NiH_4 is 0.66 eV/ H_2 without ZPE and 0.55 eV/ H_2 with ZPE. The corresponding experimental value is 0.70 eV/ H_2 .¹⁴ The agreement is fair, if we correct for the overestimation of the H_2 dissociation energy, mentioned in Sec. III. Since the H_2 dissociation energy is overestimated by 0.1 eV, it is reasonable to assume that the desorption enthalpy is overestimated by the same amount. This gives an desorption enthalpy with ZPE of 0.65 eV per H_2 , which is close to the experimental value. The correction is a constant shift and in the following we give the uncorrected results only.

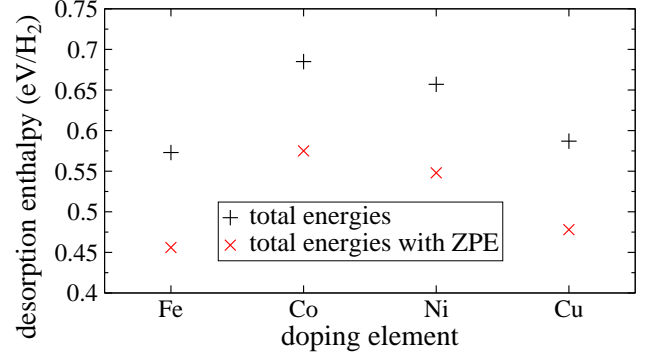


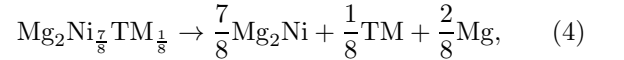
FIG. 1: (Color online) Desorption enthalpies E_{des} (eV/ H_2) of the doped hydrides.

The results for E_{des} of doped Mg_2NiH_4 are given in Fig. 1. These results clearly demonstrate that the desorption enthalpy can be tuned by an appropriate doping. The desorption enthalpy decreases considerably both for Fe and for Cu doping, i.e. by 84 and 71 meV per H_2 , respectively. However, Co doping increases the desorption enthalpy by 28 meV per H_2 . The trends for Cu and Fe doping are in qualitative agreement with experimental data.^{32,38,41}

Fig. 1 also shows the calculated desorption enthalpies corrected with ZPEs. The ZPEs of all the metals are almost identical, see Table III, and the ZPEs of the hydrides scale linearly with amount of hydrogen atoms. This means that the ZPE per hydrogen atom is almost constant and independent of the dopant atom. Therefore, the ZPE correction to the desorption enthalpy per H_2 is 0.1 eV for all compounds studied.

C. Stability

Doped Mg_2NiH_4 is stable in thin films.⁴² In order to assess whether kinetics plays an important role in stabilizing these compounds, we study the thermodynamic stability of the doped materials with respect to phase segregation. For the dehydrogenated doped Mg_2Ni metal we consider decomposition into Mg_2Ni , bulk magnesium and bulk doping metal.



where TM = Fe, Co, or Cu. Fully hydrogenated undoped Mg_2NiH_4 is compared to bulk nickel and MgH_2 . For the hydrogenated doped Mg_2NiH_4 we consider decomposition into phase segregated Mg_2NiH_4 and Mg_2FeH_6 or Mg_2CoH_5 .



with x as in Table III, and $y = 5, 6$ for Co, Fe, respectively. Since Mg_2CuH_3 is unstable with respect to decomposition into MgH_2 and MgCu_2 , we consider for the

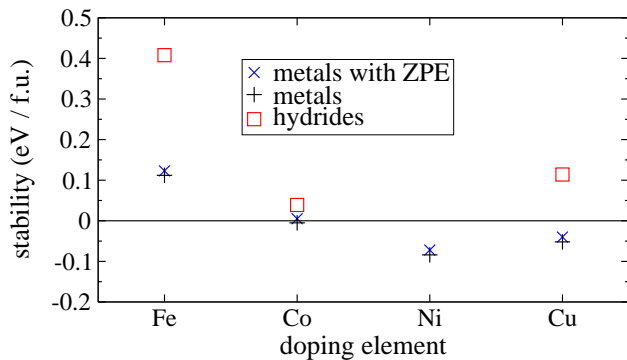
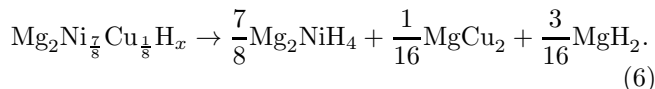


FIG. 2: (Color online) Stability with respect to phase segregation (eV / f.u.). Values are negative if the compound is stable, see Eqs. (4)-(6)

hydrogenated Cu doped Mg_2NiH_4 the possible decomposition reaction



The results are shown in Fig. 2.

Fe doped Mg_2Ni is thermodynamically unstable with respect to phase segregation into Mg_2Ni bulk Mg and bulk Fe. Co doped Mg_2Ni is a marginally unstable material in which segregation is favored by only ~ 0.01 eV per formula unit. Fe, Co doped Mg_2NiH_4 are thermodynamically unstable with respect to segregation into Mg_2NiH_4 and Mg_2FeH_6 , Mg_2CoH_5 , respectively. Doping of Mg_2Ni with Cu leads to a stable material. Experimental work proved the stability of $\text{Mg}_2\text{Ni}_{1-x}\text{Cu}_x$ solid solutions;^{32,40} for $0 < x < 0.85$ these compounds are isostructural with Mg_2Ni . Experiment indicates that the hydrogenated phase decomposes into MgH_2 , MgCu_2 and Mg_2NiH_4 .³² This is confirmed by our calculations, see Fig. 2.

In conclusion, many of the doped phases are thermodynamically unstable. This does not need to hamper their usefulness, however, since kinetics plays an important role in stabilizing the doped compounds. The hydrogen desorption temperature lies far below the temperatures that is used to anneal these materials.⁴² The Cu doped Mg_2Ni metal is thermodynamically stable, and hydrogenating this material can lead to a useful metastable compound.

V. OPTICAL PROPERTIES

The imaginary part of the dielectric function and the electronic density of states (DOS) of undoped Mg_2NiH_4 are shown in Figs. 3 and 4, respectively. They are in good agreement with the results of previous calculations.^{19,20} We find an indirect band gap of 1.6 eV and an optical gap of 1.7 eV. This is in good agreement with the experimen-

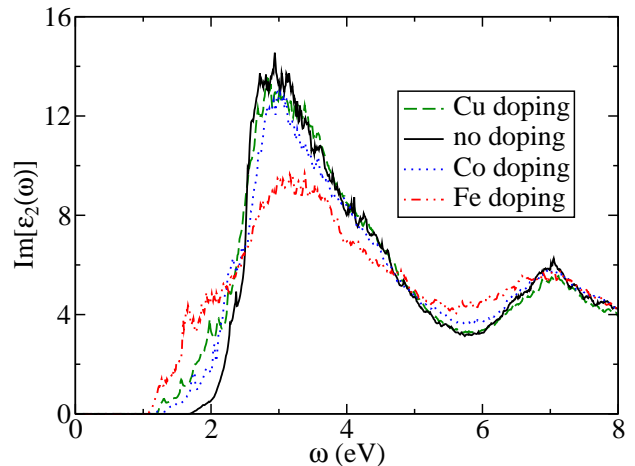


FIG. 3: (Color online) Imaginary part of the frequency dependent dielectric functions of doped Mg_2NiH_4 .

tal optical gap of 1.7 to 2.0 eV.^{25,26,27} The agreement is in fact remarkable since DFT usually underestimates the band gap by 30-50%. The dielectric function of Mg_2NiH_4 has two peaks, which can be directly related to the two peaks in the DOS of the valence bands.

The dielectric functions of doped Mg_2NiH_4 are also shown in Fig. 3. Doping alters the dielectric function and, remarkably, the size of the change correlates with the change in hydrogen desorption enthalpy caused by the dopants, see Fig. 1. This can be explained by noticing that both changes have a common cause. The changes in desorption enthalpy are due to changes in metal-hydrogen bond lengths and bond energies. Changes in bond energies shift the energy levels and hence can be detected in the optical spectrum. Such changes are largest in Fe doped Mg_2NiH_4 . An Fe dopant atom includes two extra hydrogen atoms. It gives the largest perturbation in the Mg_2NiH_4 lattice, with almost half of the metal-hydrogen bond lengths being changed with respect to the undoped case.

The DOS of doped Mg_2NiH_4 is given in Figure 4. To facilitate an internal comparison the DOS of all compounds is aligned at the bottom of the valence band. Besides the fundamental gap between the valence and conduction bands, we can identify a clear gap in the valence bands, between 2.4 and 3.6 eV below the Fermi level in undoped Mg_2NiH_4 . The states above this valence gap have a strong metal *d* character, whereas the lower valence states have a dominant hydrogen character. Cu and Fe doping introduces states in the valence gap, whereas all dopants introduce states in the fundamental gap. In the case of Cu doping these appear near the top of the valence band, whereas for Co and Fe doping gap states appear near the bottom of the conduction band. Since we have adjusted the amount of hydrogen upon doping, all doped materials are semiconducting.

The DOS can be used to interpret the dielectric func-

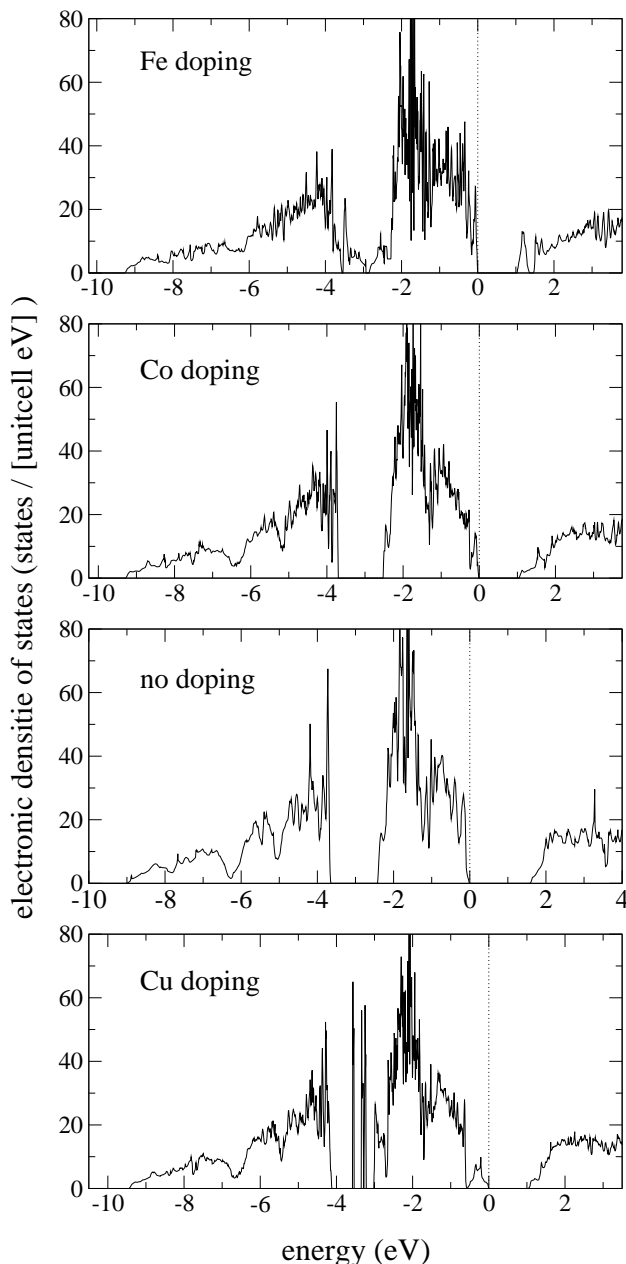


FIG. 4: Electronic densities of state of the doped and hydrides. The Fermi level is at the top of the valence bands. The four DOSs are aligned at the bottom of the valence band.

tions. The decrease in the fundamental gap in the DOS upon doping gives a decrease in the optical gaps. The largest changes in the dielectric function are observed upon Fe doping. The highest peak decreases as compared to the undoped case and the valley between the two peaks is less deep. In addition, a distinct shoulder appears at low energy. Fe doping gives a clear peak in the DOS at the bottom of the conduction band, which yields the distinct shoulder in the dielectric function. The two main peaks in the dielectric functions are not shifted upon dop-

ing. This indicates that the dopants mainly give rise to additional features via the introduction of gap states, as can be observed in the DOS. Similar conclusions hold for the Cu and Co doped cases, but the perturbation of the Mg_2NiH_4 DOS caused by doping is smaller than for the Fe doped case.

VI. CONCLUSIONS

Mg_2NiH_4 is a promising hydrogen storage material with fast (de)hydrogenation kinetics. Its hydrogen desorption enthalpy, however, is too large for practical applications. In this paper we study the effects of transition metal doping by first-principles density functional theory calculations. We show that the hydrogen desorption enthalpy can be reduced by 0.1 eV/ H_2 if one in eight Ni atoms is replaced by Cu or Fe. Replacing Ni by Co atoms, however, increases the hydrogen desorption enthalpy. We study the thermodynamic stability of the dopants in the hydrogenated and dehydrogenated phases. Doping with Co or Cu leads to marginally stable compounds, whereas doping with Fe leads to an unstable compound. The optical response of Mg_2NiH_4 is also substantially affected by doping. The optical gap in Mg_2NiH_4 is ~ 1.7 eV. Doping with Co, Fe or Cu leads to impurity bands that reduce the optical gap by up to 0.5 eV.

We study the effects of transition metal doping on the hydrogen desorption enthalpy and the optical properties of Mg_2NiH_4 by first-principles DFT calculations. The desorption enthalpy is reduced by 84 meV per H_2 , if one in eight Ni atoms is replaced by an Fe atom. Replacing one in eight Ni atoms by a Cu atom reduces the desorption enthalpy by 71 meV/ H_2 , but replacement by a Co atom increases it by 28 meV/ H_2 . Including energy corrections due to the zero point motions of the atoms changes the absolute values of the desorption energies by 0.1 eV/ H_2 . Since however the zero point energies per hydrogen atom are almost independent of the compound studied, the relative values of the desorption energies are not affected.

The thermodynamic stabilities of the doped dehydrogenated Mg_2Ni and the fully hydrogenated Mg_2NiH_4 compounds are studied by considering possible decomposition reactions. The results show that Cu doped Mg_2Ni is stable, Co doped Mg_2Ni is marginally stable, and Fe doped Mg_2Ni is unstable with respect to phase separation into Mg_2Ni , bulk Mg and the bulk transition metal dopant. The doped hydrogenated Mg_2NiH_4 compounds are either marginally unstable in the case of Co or Cu doping, or, in the case of Fe doping, clearly unstable. Kinetic barriers could be sufficiently high to stabilize metastable doped compounds since the hydrogen desorption temperatures are smaller than the temperatures used to anneal these materials. Nevertheless, thermodynamics indicates that Cu is the most promising candidate to lower the hydrogen desorption enthalpy of Mg_2NiH_4 .

By calculating the dielectric function within the ran-

dom phase approximation we study the effects of doping on the optical properties of Mg_2NiH_4 . The changes in the dielectric function can be interpreted in terms of the electronic densities of states of the corresponding compounds. The dopant atoms introduce states in the fundamental gap, as well as below the valence Ni d -band. These states cause a shift in the onset of absorption to lower energy by up to 0.5 eV and they decrease the relative heights of the peaks in the Mg_2NiH_4 absorption spectrum. The sizes of these changes correlate with the change in the hydrogen desorption enthalpy caused by the dopants. Fe doping causes the largest disruption in the Mg_2NiH_4 lattice, and the largest change in the optical properties.

Acknowledgments

The authors wish to thank R. A. de Groot (FOM) and R. Griessen (Vrije Universiteit Amsterdam) for helpful discussions and G. Kresse (University of Vienna) for use of the optical package. This work is part of the research programs of ‘Advanced Chemical Technologies for Sustainability (ACTS)’ and the ‘Stichting voor Fundamenteel Onderzoek der Materie (FOM)’, both financially supported by ‘Nederlandse Organisatie voor Wetenschappelijk Onderzoek (NWO)’.

- ¹ A. Zuttel, *Naturwissenschaften* **91**, 157 (2004).
- ² J. F. Stampfer, C. E. Holley, and J. F. Suttle, *J. Am. Chem. Soc.* **82**, 3504 (1960).
- ³ B. Bogdanovic and B. Spliethoff, *Int. J. Hydrog. Energy* **12**, 863 (1987).
- ⁴ M. Bortz, B. Bertheville, K. Yvon, E. A. Movlaev, V. N. Verbetsky, and F. Fauth, *J. Alloy. Compd.* **279**, L8 (1998).
- ⁵ G. Liang, J. Huot, S. Boily, A. V. Neste, and R. Schulz, *J. Alloy. Compd.* **291**, 295 (1999).
- ⁶ S. Bouaricha, J. P. Dodelet, D. Guay, J. Huot, S. Boily, and R. Schulz, *J. Alloy. Compd.* **297**, 282 (2000).
- ⁷ G. Liang, J. Huot, S. Boily, A. V. Neste, and R. Schulz, *J. Alloy. Compd.* **297**, 261 (2000).
- ⁸ H. Y. Leng, T. Ichikawa, S. Hino, N. Hanada, S. Isobe, and H. Fujii, *J. Phys. Chem. B* **108**, 8763 (2004).
- ⁹ J. J. Reilly and R. H. Wiswall, *Inorg. Chem.* **7**, 2254 (1968).
- ¹⁰ K. Yvon, J. Schefer, and F. Stucki, *Inorg. Chem.* **20**, 2776 (1981).
- ¹¹ D. Noreus and P. E. Werner, *Mater. Res. Bull.* **16**, 199 (1981).
- ¹² J. L. Soubeyroux, D. Fruchart, A. Mikou, M. Pezat, and B. Darriet, *Mater. Res. Bull.* **19**, 1119 (1984).
- ¹³ P. Zolliker, K. Yvon, J. D. Jorgensen, and F. J. Rotella, *Inorg. Chem.* **25**, 3590 (1986).
- ¹⁴ M. L. Post and J. J. Murray, *J. Less-common. Metals* **134**, 15 (1987).
- ¹⁵ K. J. Zeng, T. Klassen, W. Oelerich, and R. Bormann, *J. Alloy. Compd.* **283**, 151 (1999).
- ¹⁶ M. S. Liao and Q. E. Zhang, *Inorg. Chem.* **36**, 396 (1997).
- ¹⁷ G. N. Garcia, J. P. Abriata, and J. O. Sofo, *Phys. Rev. B* **59**, 11746 (1999).
- ¹⁸ G. N. Garcia, J. P. Abriata, and J. O. Sofo, *Phys. Rev. B* **65**, 064306 (2002).
- ¹⁹ U. Haussermann, H. Blomqvist, and D. Noreus, *Inorg. Chem.* **41**, 3684 (2002).
- ²⁰ W. R. Myers, L. W. Wang, T. J. Richardson, and M. D. Rubin, *J. Appl. Phys.* **91**, 4879 (2002).
- ²¹ T. J. Richardson, J. L. Slack, R. D. Armitage, R. Kostecki, B. Farangis, and M. D. Rubin, *Appl. Phys. Lett.* **78**, 3047 (2001).
- ²² W. Lohstroh, R. J. Westerwaal, B. Noheda, S. Enache, I. A. M. E. Giebels, B. Dam, and R. Griessen, *Phys. Rev. Lett.* **93**, 197404 (2004).
- ²³ W. Lohstroh, R. J. Westerwaal, J. L. M. van Mechelen, C. Chacon, E. Johansson, B. Dam, and R. Griessen, *Phys. Rev. B* **70**, 165411 (2004).
- ²⁴ J. Isidorsson, I. A. M. E. Giebels, R. Griessen, and M. Di Vece, *Appl. Phys. Lett.* **80**, 2305 (2002).
- ²⁵ D. Lupu, R. Grecu, and S. I. Farcas, *Z. Phys. Chemie-Int. J. Res. Phys. Chem. Chem. Phys.* **181**, 143 (1993).
- ²⁶ P. Selvam, B. Viswanathan, and V. Srinivasan, *J. Electron Spectrosc. Relat. Phenom.* **46**, 357 (1988).
- ²⁷ D. Lupu, R. Sarbu, and A. Biris, *Int. J. Hydrog. Energy* **12**, 425 (1987).
- ²⁸ W. Lohstroh, R. Westerwaal, J. van Mechelen, H. Schreuders, B. Dam, and R. Griessen, *J. Alloy. Compd.* **430**, 13 (2007).
- ²⁹ M. D. Vece, A. M. J. van der Eerden, D. Grandjean, R. J. Westerwaal, W. Lohstroh, S. G. Nikitenko, J. J. Kelly, and D. C. Koningsberger, *Mater. Chem. Phys.* **91**, 1 (2005).
- ³⁰ R. J. Westerwaal, M. Slaman, C. P. Broedersz, D. M. Borsa, B. Dam, R. Griessen, A. Borgschulte, W. Lohstroh, B. Kooi, G. ten Brink, et al., *J. Appl. Phys.* **100**, 063518 (2006).
- ³¹ M. Pasturel, M. Slaman, D. M. Borsa, H. Schreuders, B. Dam, R. Griessen, and W. Lohstroh, *Appl. Phys. Lett.* **89**, 021913 (2006).
- ³² J. Darnaudery, M. Pezat, and B. Darriet, *J. Less-Common Met* **92**, 199 (1983).
- ³³ Y. Q. Lei, Y. M. Wu, Q. M. Yang, J. Wu, and Q. D. Wang, *Z. Phys. Chemie-Int. J. Res. Phys. Chem. Chem. Phys.* **183**, 379 (1994).
- ³⁴ D. L. Sun, Y. Q. Lei, W. H. Liu, J. J. Jiang, J. Wu, and Q. D. Wang, *J. Alloy. Compd.* **231**, 621 (1995).
- ³⁵ K. Ikeda, S. Orimo, A. Zuttel, L. Schlapbach, and H. Fujii, *J. Alloy. Compd.* **280**, 279 (1998).
- ³⁶ G. Liang, S. Boily, J. Huot, A. V. Neste, and R. Schulz, *Mater. Sci. Forum.* **269-2**, 1049 (1998).
- ³⁷ J. L. Bobet, E. Akiba, Y. Nakamura, and B. Darriet, *Int. J. Hydrog. Energy* **25**, 987 (2000).
- ³⁸ J. L. Bobet, E. Grigorova, M. Khrussanova, M. Khrisov, D. Radev, and P. Peshev, *J. Alloy. Compd.* **345**, 280 (2002).
- ³⁹ T. Sato, H. Blomqvist, and D. Noreus, *J. Alloy. Compd.* **356**, 494 (2003).
- ⁴⁰ L. Q. Li, I. Saita, K. Saito, and T. Akiyama, *J. Alloy. Compd.* **372**, 218 (2004).

- ⁴¹ M. V. Simicic, M. Zdujic, R. Dimitrijevic, L. Nikolic-Bujanovic, and N. H. Popovic, *J. Power Sources* **158**, 730 (2006).
- ⁴² W. Lohstroh private communication.
- ⁴³ G. Kresse and D. Joubert, *Phys. Rev. B* **59**, 1758 (1999).
- ⁴⁴ P. E. Blöchl, *Phys. Rev. B* **50**, 17953 (1994).
- ⁴⁵ G. Kresse and J. Furthmüller, *Phys. Rev. B* **54**, 11169 (1996).
- ⁴⁶ G. Kresse and J. Furthmüller, *Comput. Mater. Sci.* **6**, 15 (1996).
- ⁴⁷ G. Kresse and J. Hafner, *Phys. Rev. B* **47**, 558 (1993).
- ⁴⁸ J. P. Perdew, J. A. Chevary, S. H. Vosko, K. A. Jackson, M. R. Pederson, D. J. Singh, and C. Fiolhais, *Phys. Rev. B* **46**, 6671 (1992).
- ⁴⁹ S. G. Louie, S. Froyen, and M. L. Cohen, *Phys. Rev. B* **26**, 1738 (1982).
- ⁵⁰ G. Kresse, J. Furthmüller, and J. Hafner, *Europhys. Lett.* **32**, 729 (1995).
- ⁵¹ M. Gajdos, K. Hummer, G. Kresse, J. Furthmüller, and F. Bechstedt, *Phys. Rev. B* **73**, 045112 (2006).
- ⁵² P. E. Blöchl, O. Jepsen, and O. K. Andersen, *Phys. Rev. B* **49**, 16223 (1994).
- ⁵³ H. J. Monkhorst and J. D. Pack, *Phys. Rev. B* **13**, 5188 (1976).
- ⁵⁴ P. Zolliker, K. Yvon, J. Jorgensen, and F. J. Rotella, *Inorg. Chem.* **25**, 3590 (1986).
- ⁵⁵ P. Zolliker, K. Yvon, P. Fischer, and J. Scheffer, *Inorg. Chem.* **24**, 4177 (1985).
- ⁵⁶ J. Didisheim, P. Zolliker, K. Yvon, P. Fischer, J. Scheffer, M. Gubelmann, and A. Williams, *Inorg. Chem.* **23**, 1953 (1984).
- ⁵⁷ M. J. van Setten, G. A. de Wijs, V. A. Popa, and G. Brocks, *Phys. Rev. B* **72**, 073107 (2005).
- ⁵⁸ R. C. Weast and M. J. Astle, *CRC Handbook of Chemistry and Physics* (CRC press, New York, 1982), 62nd ed.
- ⁵⁹ K. Huber and G. Herzberg, *Molecular Spectra and Molecular Structure*, vol. IV Constants and diatomic molecules (Van Nostrand Reinhold Company, 1979).